

Activation of cAMP-dependent Cl⁻ currents in guinea-pig Paneth cells without relevant evidence for CFTR expression

Takehiko Tsumura*, Akihiro Hazama, Takashi Miyoshi, Shunji Ueda*
and Yasunobu Okada

*Department of Cellular and Molecular Physiology, National Institute for Physiological Sciences, Okazaki 444-8585 and *Department of Internal Medicine, Kyoto University Faculty of Medicine, Kyoto 606-8501, Japan*

(Received 14 April 1998; accepted after revision 20 July 1998)

1. To determine whether Paneth cells exhibit functional expression of cAMP-activated Cl⁻ currents and molecular expression of the cystic fibrosis transmembrane conductance regulator (CFTR), we applied whole-cell patch clamp and single-cell mRNA analysis by reverse transcription (RT) followed by polymerase chain reaction (PCR) amplification to single Paneth cells in crypts isolated from the guinea-pig small intestine.
2. Prominent activation of Cl⁻ currents was consistently observed after stimulation with dibutyryl cAMP and forskolin or with vasoactive intestinal polypeptide (VIP). The cAMP-activated Cl⁻ current was inhibited by removal of intracellular ATP or administration of an inhibitor of protein kinase A.
3. Many of the biophysical and pharmacological properties of the currents were phenotypically similar to those of the CFTR Cl⁻ channel, such as the ohmic current–voltage relationship, the anion selectivity with a Type III sequence (Br⁻ > Cl⁻ > I⁻ ≫ F⁻ ≧ gluconate⁻), I⁻-induced blockage, insensitivity to a stilbene-derivative Cl⁻ channel blocker, and sensitivity to a carboxylate analogue Cl⁻ channel blocker. The sensitivity of the current to glibenclamide was, however, much weaker than that reported for the CFTR Cl⁻ channel current. In contrast to the time independence of CFTR currents, the inward component of the Paneth cell Cl⁻ currents exhibited inactivation kinetics.
4. Expression of CFTR mRNA could not be detected by RT-PCR analysis in almost all single Paneth cells, although its expression was consistently detected at the whole-crypt level. The presence of a small number of CFTR-expressing epithelial cells, which were scattered both in villi and crypts but not at the crypt base where Paneth cells were located, was demonstrated by immunocytochemistry.
5. Taken together, it appears that guinea-pig Paneth cells functionally express cAMP-activated Cl⁻ conductance without relevant evidence for molecular expression of CFTR. Functional expression of VIP receptors in the Paneth cells was also demonstrated.

Paneth cells are granulated secretory epithelial cells located at the base of the crypts of Lieberkühn in the small intestine of most mammalian species. Since Paneth cells release granules, which contain lysozyme, immunoglobulin, phospholipase A₂, α₁-antitrypsin and α-defensins termed cryptidins, into the lumen of the crypts, Paneth cells are thought to play a key role in host defence (Ouellette, 1997).

In the small intestine the crypt compartment has been postulated to be the site of salt and fluid secretion (Sullivan & Field, 1991), though the evidence is still highly circumstantial. The undifferentiated epithelial cells lining the crypt are thought to be the intestinal Cl⁻-secreting cells and actually have been shown to depolarize in response to

vasoactive intestinal polypeptide (VIP) or forskolin in isolated guinea-pig crypts (Walters *et al.* 1992). Recently, Paneth cells located at the crypt base adjacent to these undifferentiated intestinal epithelial cells (enterocytes) have been suggested to be involved in small intestinal Cl⁻ secretion by releasing cryptidins which may selectively permeabilize the apical membrane of undifferentiated enterocytes (Lencer *et al.* 1997). However, no study has been performed to test the possibility that Paneth cells themselves may possess the Cl⁻ conductance.

The cystic fibrosis transmembrane regulator (CFTR) gene codes for a cAMP-activated Cl⁻ channel expressed in the apical membrane of many epithelial cells (Fuller & Benos,

1992). The expression of CFTR mRNA was shown by *in situ* hybridization in the rat (Treize & Buchwald, 1991) and human (Strong *et al.* 1994) small intestine, and the expression of the CFTR protein was shown by immunocytochemistry in the human duodenum (Hoogeveen *et al.* 1991) and jejunum (Crawford *et al.* 1991). However, CFTR expression in single Paneth cells has not been intensively examined.

CFTR-like cAMP-activated Cl^- currents have consistently been recorded from the human colonic epithelial cell lines T₈₄ (Tabcharani *et al.* 1990) and Caco-2 (Bear & Reyes, 1992). In contrast, there has been no report of CFTR-like Cl^- current recordings from mammalian small intestinal enterocytes, including Paneth cells, although cAMP-independent Cl^- currents were recorded from villus enterocytes isolated from guinea-pig small intestine (Sepúlveda *et al.* 1991) and cAMP-dependent depolarization was observed in the guinea-pig enterocytes located at the upper portion of the isolated crypt (Walters *et al.* 1992).

The aims of the present study were to record cAMP-activated Cl^- currents by whole-cell patch clamp and to assess the molecular expression of CFTR using single-cell reverse transcription-polymerase chain reaction (RT-PCR) and immunocytochemical techniques in guinea-pig Paneth cells in isolated crypts. A preliminary account of part of these data has appeared in abstract form (Tsumura *et al.* 1997).

METHODS

Isolation of crypts and villi

Intestinal epithelial fragments were sequentially isolated along the villus crypt axis by a vibration- Ca^{2+} -chelation technique, as described by McNicholas *et al.* (1994). Briefly, a 15-cm-long segment of proximal small intestine was excised from adult male guinea-pigs under anaesthesia with ether, and the animals were then killed by cervical dislocation before they recovered consciousness. All experiments complied with the Institutional Guidelines for the Care and Use of Laboratory Animals. After being flushed with ice-cold saline (0.9% NaCl), the segment was everted on a glass spiral and vibrated at 50 Hz at room temperature (23–26 °C) in isolation solution which contained (mM): 112 NaCl, 5 KCl, 0.5 dithiothreitol (DTT), 30 Na₂EDTA, 15 Hepes and 10 Tris (pH 7.1). This isolation solution was replaced by fresh solution at 30 min intervals, up to six times. Collected fractions were washed with ice-cold storage solution which was composed of (mM): 137.5 sodium gluconate, 4.2 potassium gluconate, 2 MgCl₂, 20 mannitol, 2.9 calcium gluconate, 0.5 hydroxybutyrate, 8 Hepes and 6 Na-Hepes (pH 7.4), plus 1 mg ml⁻¹ bovine serum albumin (BSA).

Under a phase-contrast or differential interference microscope, fractions 1–3 were found to contain mainly upper villus fragments, fraction 4 contained fragments consisting of both lower villi and upper or whole crypts, and fractions 5 and 6 contained fragments mainly consisting of lower or whole crypts. These fractions were kept on ice until use. The crypt-rich fractions were used for both electrophysiological and immunocytochemical studies, and other fractions were used for immunocytochemistry. For immunoprecipitation studies, the fractions were combined.

Patch-clamp whole-cell recordings

Isolated crypts were placed in a chamber (0.5 ml) and perfused with extracellular solution. In some experiments crypts were used after being stained with Neutral Red (30 µg ml⁻¹, 30 min). This vital staining did not affect the basal and cAMP-activated currents. In several experiments, to observe the effects of closure of the crypt open end, crypts were used after their open ends were tied off with thread (1 µm in diameter).

Whole-cell recordings were carried out as previously described (Tsumura *et al.* 1996), from granular enterocytes (which had been identified as Paneth cells) located at the base of isolated crypts. In contrast to neighbouring distal undifferentiated enterocytes, mouse Paneth cells are known to lack gap junctions (Bjerknes *et al.* 1985). In fact, in preliminary fluorescence microscope studies in guinea-pig crypts, Lucifer Yellow (100 µM) incorporated in the patch pipette was not found to transfer to adjacent cells from a Paneth cell under whole-cell conditions ($n=4$). Thus, Paneth cells are suitable for whole-cell voltage clamp due to negligible electrical cell-to-cell coupling. After compensation for the series resistance (5–25 MΩ) and cell capacitance (4–10 pF), membrane currents were measured using an Axopatch 200A amplifier (Axon Instruments, Foster City, CA, USA). To monitor the time course of current activation and recovery, alternating step pulses (1 s duration) to ± 40 mV were routinely applied from a holding potential of 0 mV every 7.5 s. The current–voltage (I – V) curves were obtained by step pulses (0.5 s duration) from –100 to +100 mV in 20 mV increments or by ramp voltage clamp from –100 to +100 mV or –80 to +80 mV for 1.2 s. The amplitude of the instantaneous current was measured at 2.5 ms after the step onset. Junction potentials were measured with a 150 mM KCl bridge and were compensated in studies of anion selectivity. Anion permeability ratios were derived from reversal potentials (V_{rev}) obtained from I – V plots using the Hodgkin–Katz modification of the Goldman equation. Current signals were filtered and digitized at 1 and 2.5 kHz, respectively. The time course of hyperpolarization-induced inactivation of cAMP-activated Cl^- current was well fitted by a double exponential function, and thus the steady-state current level was simultaneously evaluated. pCLAMP software (version 6.0.2; Axon Instruments) was used for command pulse control, data acquisition and analysis.

The bath NaCl or KCl solution contained (mM): 150 NaCl or KCl, 1 CaSO₄, 10 mannitol, 15 Hepes and 10 Tris (pH 7.5). To reduce the extracellular Cl^- concentration ($[\text{Cl}^-]_o$), 100 or 135 mM KCl was replaced with 200 or 270 mM mannitol (or 135 mM potassium gluconate). To elevate intracellular [cAMP], both dibutyryl cAMP (db-cAMP) and forskolin were added to the extracellular solution. The pipette (intracellular) solution contained (mM): 150 NaCl (or KCl), 3 MgATP, 5 BAPTA, 15 mannitol, 10 Hepes and 10 Tris (pH 7.4). When stimulated with VIP or secretin added to the bathing solution, GTP (50 µM), GTPγS (100 µM) or GDPβS (100 µM) was added to the pipette solution. To examine anion selectivity, 150 mM KCl in the bath KCl solution was replaced with 150 mM KBr, KI, KF or potassium gluconate. To elevate intracellular [cAMP] in Paneth cells in crypts the open ends of which had been tied off, cAMP stimulants were added to the bathing solution prior to attaching the patch pipette to the cell, because stimulant application by bath perfusion resulted in mechanical movement of the crypts tied off with the thread, thereby interfering with patch-clamp experiments.

Forskolin, db-cAMP, cAMP, porcine VIP, porcine secretin, GTPγS, GDPβS, glibenclamide, 4,4'-diisothiocyanostilbene-2,2'-disulphonic acid (DIDS) and diphenylamine-2-carboxylic acid (DPC) were

purchased from Sigma; *N*-[2-(*p*-bromocinnamylamino)ethyl]-5-isoquinolinesulphonamide (H-89), as well as its derivative *N*-[2-(*N*-formyl-*p*-chlorocinnamylamino)ethyl]-5-isoquinolinesulphonamide (H-85), were from Seikagaku Corporation (Tokyo, Japan). 5-Nitro-2-(3-phenylpropylamino)-benzoic acid (NPPB) was a generous gift from Dr M. Kuno (Shionogi Pharmaceutical Co., Osaka, Japan). The vehicles for stock solutions were ethanol for forskolin and DMSO for H-89 and the Cl^- channel blockers. Ethanol and DMSO alone did not affect whole-cell currents at the final concentrations used (less than 0.04 and 0.2%, respectively).

All patch-clamp studies were performed at 37 ± 1 °C. Electrophysiological data are given as means \pm S.E.M. of observations for *n* cells. Statistical differences of the data were evaluated by Student's paired or unpaired *t* test and considered significant at $P < 0.05$.

RT-PCR study at the whole-crypt level

Poly(A)⁺ RNA was extracted from isolated crypts with Magnetic Porous Glass (MPG) Direct mRNA Purification Kit (CPG Inc., NJ, USA). In brief, the cells were lysed in extraction-hybridization buffer (100 mM Tris-HCl, 500 mM LiCl, 10 mM EDTA, 1% lithium dodecylsulphate (LiDS), 5 mM DTT, pH 8.0) and the poly(A)⁺ RNA was hybridized with MPG streptavidin plus biotinylated oligo(dT)₂₅. The poly(A)⁺ RNA was washed three times with 500 μ l of washing buffer (10 mM Tris-HCl, 150 mM LiCl, 1 mM EDTA, 0.1% LiDS, pH 8.0). Then the poly(A)⁺ RNA was collected

magnetically and eluted with 20 μ l of 2 mM EDTA solution.

The primers corresponding to the regulatory (R) domain (Diamond *et al.* 1991) of guinea-pig CFTR were synthesized on an automated DNA synthesizer. To increase the specificity and sensitivity of the PCR for the CFTR gene, we used nested primers. The sequences of the primers were 5'-TGGTCACTTCTAAAATGGAAC-3' and 5'-GTTATCAGGTTCAACACCGAC-3' (outer pair, 5' and 3', respectively: the amplified fragment corresponds to nucleotides 1937 to 2453 of the human CFTR cDNA sequence) and 5'-CCTGTGGAGAGAAGACTGTCC-3' and 5'-CACCGACTGTCTCCTACTGC-3' (inner pair, 5' and 3', respectively: the amplified fragment corresponds to nucleotides 2323 to 2439 of the human CFTR cDNA sequence). The expected size of the amplified fragment by the second PCR was 114 bp. As a positive control we amplified a fragment of mRNA of glyceraldehyde 3-phosphate dehydrogenase (G-3-PDH) by single PCR. The sequences of the primers (Clontech, Palo Alto, CA, USA) were 5'-ACCACA GTCCATGCCATCAC-3' and 5'-TCCACCACCCTGTTGATGTA-3'. The resulting PCR product using these primers was 452 bp. The reverse transcription and PCR were performed as described by Rappolee *et al.* (1988), using the Superscript Preamplification System for First Strand cDNA Synthesis (Gibco BRL) and Ampli Taq Gold (Perkin Elmer, Norwalk, CT, USA). The PCR programme for the first amplification with the outer primer pair of CFTR was as follows: 12 min preheating for

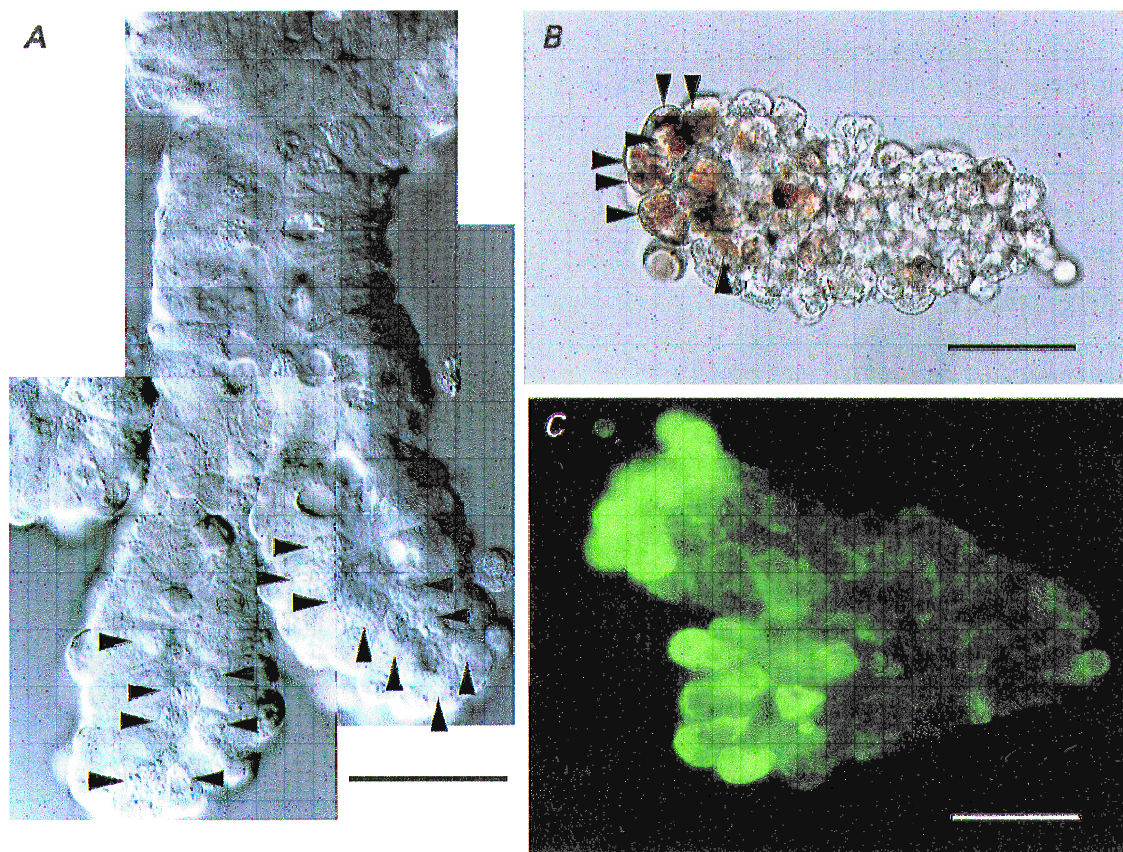


Figure 1. Morphological identification of Paneth cells

Micrographs of the crypts isolated from the guinea-pig small intestine. *A*, differential interference micrograph. Numerous granules (arrowheads) could be seen at the supranuclear to apical portion in the enterocytes near the base of crypts. *B*, light micrograph. Crypt base enterocytes (arrowheads) contained granules preferentially reactive to Neutral Red. *C*, immunofluorescence micrograph. The crypt base enterocytes were reactive to anti-lysozyme antibody. Scale bars, 30 μ m.

the activation of Ampli Taq Gold at 94 °C, followed by thirty-three PCR cycles at 94 °C (1 min)/57 °C (2 min)/72 °C (3 min), and 10 min final elongation at 72 °C. Aliquots (2 μ l) of this PCR product were subjected to the second-stage amplification with the inner primer pair by thirty-three PCR cycles at 94 °C (1 min)/61 °C (2 min)/72 °C (3 min). The PCR programme for G-3-PDH was the same as that of the first-stage amplification for CFTR. The cDNA amount of the sample was measured by a spectrophotometer (DU640; Beckman, Palo Alto, CA, USA). For each PCR, signal was never detected from reaction buffer alone (without containing sample cDNA).

RT-PCR study at the single Paneth cell level

Using the single-cell RT-PCR technique (Sucher & Deitcher, 1995), analysis of CFTR mRNA was performed in single Paneth cells. Glycogen (20 μ g ml⁻¹) was added as an mRNA carrier to the pipette solution. To obtain RNase-free conditions, glass micropipettes were heated at 240 °C for 4 h, and the pipette solution was treated with diethylpyrocarbonate (DEPC) and autoclaved. After the currents had been recorded, suction was applied to the pipette, thereby collecting the cytosol. Subsequently, the pipette tip was broken into a reaction tube, and approximately 6 μ l of KCl pipette solution was ejected by positive pressure into the reaction tube. Latex gloves were worn at all times during the procedure. The RT procedures for single Paneth cell PCR were the same as those for whole crypts. The conditions (such as annealing temperature and number of cycles) of single-cell RT-PCR were optimized by amplifying the diluted whole-crypt cDNA, as recommended by Sucher & Deitcher (1995).

Immunocytochemistry

Isolated crypts were fixed with 4% paraformaldehyde for 30–60 min, washed with phosphate-buffered saline (mm: 127 NaCl, 2.7 KCl, 8 Na₂HPO₄, 1.47 KH₂PO₄, 0.5 MgCl₂, 0.9 CaCl₂ and 20 mannitol) supplemented with 1% BSA, and treated with anti-lysozyme antibody or anti-CFTR antibody (diluted to 10 or 5 μ g ml⁻¹, respectively). Mouse polyclonal antibody against rabbit IgG was used as the secondary antibody. Secondary antibody binding was detected with fluorescein isothiocyanate (FITC)-conjugated anti-mouse IgG antibody. Rabbit anti-human lysozyme antibody was purchased from Progen Biotechnik GmbH (Heidelberg, Germany). Rabbit anti-CFTR antibodies were raised against the synthetic oligopeptide, DPVERRRLS, which corresponds to a part of the R domain of guinea-pig CFTR (corresponding to amino acids 730–737 of human CFTR), and purified by ligand affinity columns using the oligopeptides. Non-immune rabbit serum or purified rabbit IgG (Zymed, San Francisco, USA) was used as a negative control.

Immunoprecipitation

Isolated intestinal epithelia (fractions 1–6 combined) were solubilized with a buffer containing 0.1% (w/v) sodium dodecyl sulphate (SDS), 1% (v/v) Nonidet P-40, 150 mM NaCl, 1 mM EDTA and 10 mM Tris-HCl (pH 7.4) supplemented with 10 μ g ml⁻¹ aprotinin (Sigma), sonicated three times for 10 s, and then centrifuged in a microcentrifuge at 4 °C for 5 min (15 000 r.p.m.), and the pellet discarded. Solubilized proteins were incubated for 1 h at 4 °C with the anti-CFTR antibody (50 μ g ml⁻¹) or purified rabbit IgG.

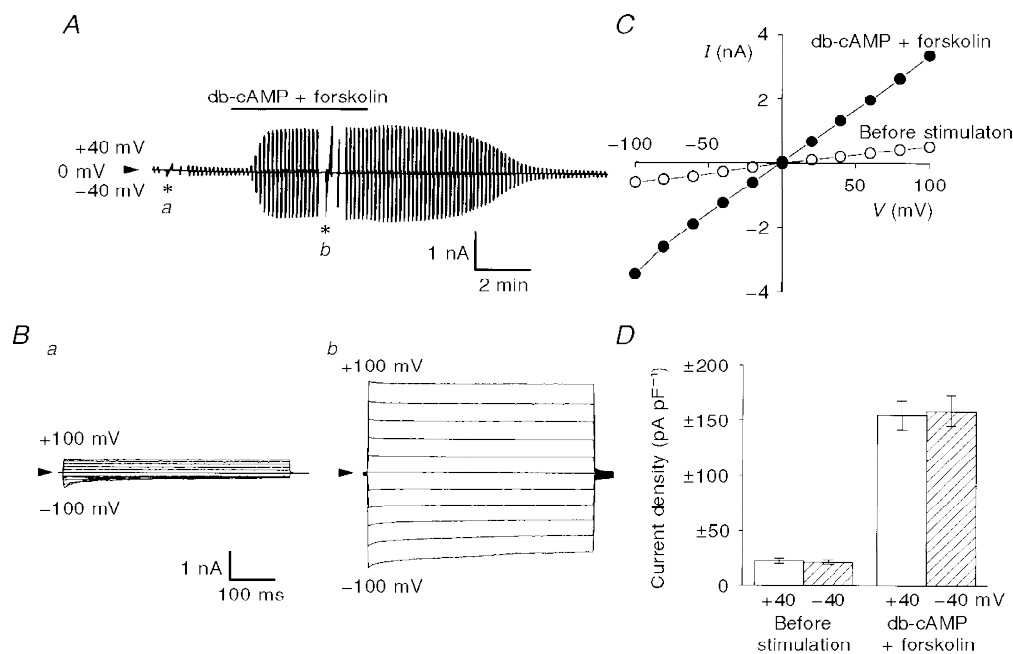


Figure 2. cAMP-induced activation of whole-cell currents

Whole-cell recordings were performed in single Paneth cells equilibrated with KCl solutions. *A*, representative record before and after stimulation with 500 μ M db-cAMP and 20 μ M forskolin (indicated by horizontal bar) during application of alternating pulses from 0 to \pm 40 mV or of step pulses from -100 to +100 mV in 20 mV increments (asterisks). The gain of the chart recorder was changed by one-half when step pulses were applied. In this and subsequent figures, arrowheads indicate the zero-current level. *B*, expanded traces of the current responses (*a* and *b* in *A*) to step pulses before (*a*) and after (*b*) cAMP stimulation. *C*, peak I - V relationships before (○) and after (●) cAMP stimulation for data shown in *B*. *D*, mean peak current density recorded at \pm 40 mV before and after cAMP stimulation. Error bars represent S.E.M. ($n = 39$).

Protein A agarose ($100 \mu\text{l ml}^{-1}$) was then added. Following a 1 h incubation at 4°C , the agarose beads were washed three times with the same buffer used for cell lysates. Immunoprecipitated samples were eluted into SDS-PAGE sample buffer containing 3% (w/v) SDS, 15% sucrose and 92.5 mM Tris-HCl (pH 6.9). Samples were heated at 95°C for 5 min and subjected to 10% SDS-PAGE. Immunoprecipitated CFTR subjected to SDS-PAGE was transferred to nitrocellulose membrane. The signals were detected using the anti-CFTR antibody and ECL kit (Amersham Life Science, Little Chalfont, UK).

RESULTS

Identification of Paneth cells in isolated crypts

A subpopulation of epithelial cells, which contained a large number of granules (indicated by arrowheads in Fig. 1A) in the supranuclear to apical portion, was found at the base of isolated crypts, using a differential interference microscope (Fig. 1A). The granules were selectively stained by Neutral Red (Fig. 1B). Immunocytochemistry showed that these granular cells at the crypt base were reactive to anti-lysozyme antibody (Fig. 1C). Taken together, it was concluded that these cells were Paneth cells and that they could easily be recognized by their location and granular content under a light microscope.

cAMP-activated Cl^- currents in Paneth cells

When Paneth cells equilibrated with intracellular and extracellular KCl solutions were stimulated with a cAMP-elevating cocktail consisting of forskolin ($20 \mu\text{M}$) and db-cAMP ($500 \mu\text{M}$) under whole-cell voltage clamp, prominent current activation was consistently achieved in a

reversible manner, as shown in Fig. 2A. The voltage dependence of cAMP-activated currents was investigated by applying step pulses from -100 to $+100 \text{ mV}$ in 20 mV increments. Both basal currents before stimulation and activated currents after stimulation showed little time or voltage dependence at positive potentials, whereas they exhibited weakly time- and voltage-dependent inactivation at potentials negative to -40 mV (Fig. 2B). The instantaneous peak I - V relationship was almost linear (Fig. 2C). The mean amplitudes of the instantaneous current density recorded at -40 and $+40 \text{ mV}$ were essentially identical, as summarized in Fig. 2D. Virtually identical cAMP-activated Cl^- currents were observed from Paneth cells in the crypt, the open end of which was closed by being tightly tied off with a fine thread, and the current density at -40 mV was $-170.7 \pm 24.8 \text{ pA pF}^{-1}$ ($n = 7$), which was not statistically different from that of the control (Fig. 2D).

The effects of partially replacing the extracellular KCl with mannitol on the I - V curves of cAMP-activated currents were examined by ramp voltage clamp in Paneth cells equilibrated with KCl solutions. As shown in Fig. 3A, the V_{rev} of the cAMP-activated component obtained after subtraction of basal currents shifted in a positive direction with decreasing extracellular $[\text{KCl}]$, indicating that the cAMP-activated component was due to an anionic conductance. The V_{rev} value shifted by $+56.2 \text{ mV}$ per 10-fold decrease in $[\text{Cl}^-]_o$ (Fig. 3A, inset), and this was close to the theoretical value for a Cl^- -selective electrode (dotted line). In contrast, the V_{rev} of basal currents largely shifted in a negative direction ($-12.5 \pm 1.6 \text{ mV}$, $n = 3$) when the extracellular KCl concentration was decreased (from 150 to

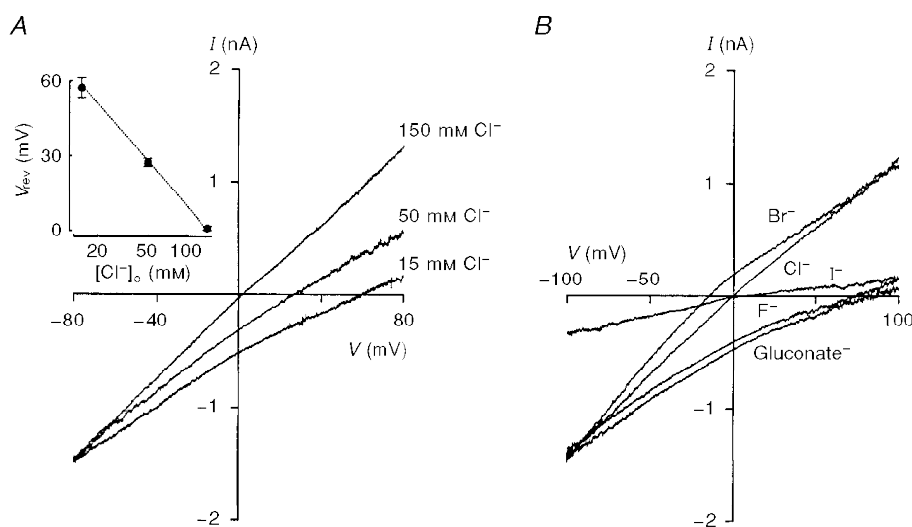


Figure 3. Anion selectivity of cAMP-activated currents

I - V curves were measured by ramp voltage clamp (from -80 or -100 to $+80$ or $+100 \text{ mV}$ for 1.2 s) in Paneth cells equilibrated with KCl solutions. Extracellular Cl^- concentrations and anion species are indicated beside the curves in A and B, respectively. Background basal currents recorded before cAMP stimulation were subtracted from currents recorded after activation. A, effects of changes in extracellular Cl^- concentration. Inset, relationship between the reversal potential (ordinate) and $[\text{Cl}^-]_o$. Each symbol represents the mean \pm s.e.m. of 4–12 observations. The dotted line represents the ideal Cl^- equilibrium potential. B, effects of anion substitution.

50 mM), indicating that a K^+ conductance predominantly contributes to the basal current recorded under these conditions. In fact, the basal current was largely abolished by totally replacing K^+ with Na^+ (see below).

The anion selectivity of the cAMP-activated current was examined in Paneth cells equilibrated with KCl solutions by replacing extracellular Cl^- with other anionic species. Representative results are shown in Fig. 3*B*. The mean V_{rev} values shifted from -0.5 ± 0.3 mV ($n = 27$) to -15.6 ± 0.9 mV ($n = 6$), 6.0 ± 1.5 mV ($n = 7$), 77.3 ± 7.0 mV ($n = 7$) and 78.6 ± 6.8 mV ($n = 7$), when Cl^- was totally replaced with Br^- , I^- , F^- and gluconate $^-$, respectively. The relative anion permeability was 1.86 ± 0.07 , 1, 0.79 ± 0.04 , 0.05 ± 0.01 and 0.04 ± 0.01 for Br^- , Cl^- , I^- , F^- and gluconate $^-$, respectively. This sequence corresponds to Eisenman's sequence Type III (Wright & Diamond, 1977). Figure 3*B* also shows a blocking effect of I^- .

Both the amplitude of the cAMP-activated Cl^- current and the inactivation kinetics were markedly affected when $[Cl^-]_o$ was reduced by replacing extracellular KCl with mannitol, as shown in Fig. 4*A*. Several minutes after reduction of $[Cl^-]_o$ peak currents were prominently diminished (Fig. 4*Ba*) despite the presence of a high concentration of intracellular Cl^- (150 mM). The time course of the hyper-

polarization-induced inactivation, which could be better fitted by a double exponential function than a single exponential function (Fig. 4*Ad*), became faster when $[Cl^-]_o$ was decreased (Fig. 4*Bb*). A plot of the ratio of steady-state to peak currents against $[Cl^-]_o$ (Fig. 4*Bc*) showed that the steady-state inactivation was augmented by reduction of the extracellular Cl^- level. Essentially identical effects were observed when extracellular KCl was replaced with potassium gluconate. When $[Cl^-]_o$ was thus reduced to 15 mM using gluconate, the peak current recorded at -80 mV decreased to $58 \pm 4\%$ of that recorded at 150 mM extracellular Cl^- (Cl^-_o) ($n = 5$), the fast and slow time constants of inactivation decreased to 18.9 ± 2.9 and 230.8 ± 52.7 ms, respectively, and the ratio of steady-state to peak currents decreased to 0.61 ± 0.05 . Therefore, it appears that not only channel activity but also inactivation gating are dependent on extracellular $[Cl^-]$.

When Paneth cells were equilibrated with NaCl solutions, the basal current recorded before stimulation was virtually abolished, as demonstrated in Fig. 5*A* (see also Figs 6*B* and 7*A*), whereas stimulation with a cAMP-elevating cocktail consistently induced current activation (Fig. 5*A*).

A stilbene-derivative Cl^- channel blocker, DIDS (500 μM), failed to block the cAMP-activated Cl^- current, as shown in

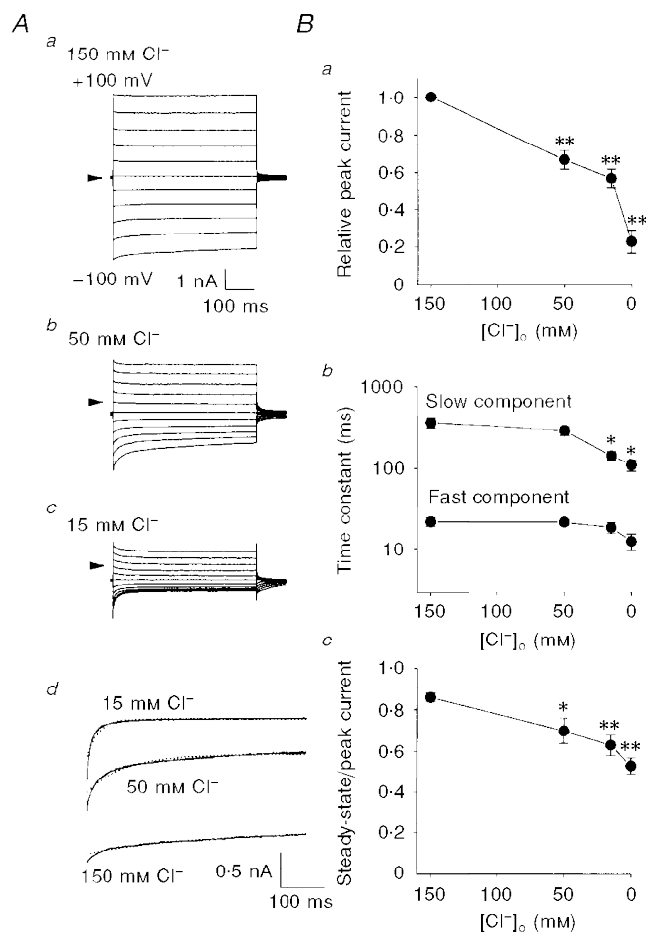


Figure 4. Extracellular $[Cl^-]$ dependence of cAMP-activated Cl^- currents

Whole-cell recordings were performed by applying step pulses (from -100 to $+100$ mV in 20 mV increments) in single Paneth cells equilibrated with KCl solutions.

A, representative traces of current responses to step pulses at $[Cl^-]_o$ of 150 (*a*), 50 (*b*) and 15 mM (*c*), and examples of double (continuous line) and single (dotted line) exponential fits to currents in response to a voltage of -80 mV at 150, 50 and 15 mM Cl^-_o (*d*). *B*, effects of changes in $[Cl^-]_o$ on the peak current relative to that recorded at 150 mM $[Cl^-]_o$ (*a*), on the time constants of inactivation (*b*) and on the ratio of steady-state current to peak current (*c*) at -80 mV. Each symbol represents the mean \pm s.e.m. of 5–20 observations. * $P < 0.05$ and ** $P < 0.01$, significantly different from the value at 150 mM Cl^-_o .

Fig. 5A (top trace) and Fig. 5Ba. A carboxylate analogue Cl^- channel blocker, NPPB ($500 \mu\text{M}$), rapidly suppressed the cAMP-activated Cl^- current in a fairly reversible manner (Fig. 5A, second trace and 5Bb). The effect was slightly voltage dependent, and the inward current was markedly more diminished than the outward current. Another carboxylate blocker, DPC (2 mM), induced immediate inhibition after administration, in a fully reversible manner (Fig. 5A, third trace). Concentration–inhibition curves (Fig. 5Bc) clearly show the voltage-dependent inhibition. The concentrations for half-maximal inhibition (IC_{50}) by DPC were 426.0 ± 33.8 , 577.0 ± 43.8 , 669.4 ± 45.2 and $698.9 \pm 50.9 \mu\text{M}$ at -80 , -40 , $+40$ and $+80 \text{ mV}$, respectively. Similar blocking effects were also rapidly induced by an antidiabetic sulfonylurea, glibenclamide ($500 \mu\text{M}$), as shown in Fig. 5A (bottom trace). The concentration dependence and voltage dependence of the glibenclamide effects are summarized in Fig. 5Bd. The IC_{50} values for the glibenclamide effect were 156.2 ± 44.2 , 288.5 ± 54.7 , 554.2 ± 105.9 and $896.2 \pm 278.0 \mu\text{M}$ at -80 , -40 , $+40$ and $+80 \text{ mV}$, respectively.

When Paneth cells were equilibrated with a pipette solution devoid of ATP, cAMP stimulation failed to induce activation of Cl^- currents, as shown in Fig. 6Aa. Even in the presence of intracellular ATP, cAMP-induced activation of Cl^- currents was largely abolished by pretreatment with an inhibitor of protein kinase A (PKA), H-89 ($10 \mu\text{M}$), for over 30 min, as shown in Fig. 6Ab. Figure 6B summarizes the effects of nominally ATP-free conditions and of pretreatment with H-89. In contrast, pretreatment with H-85 ($10 \mu\text{M}$), which is a derivative of, and a negative control for, H-89, did not affect cAMP-induced Cl^- current activation (data not shown, $n = 3$).

VIP-induced activation of Cl^- currents in Paneth cells

Since VIP is known to stimulate cAMP production via the VIP receptor coupled to adenylyl cyclase through G proteins in a number of target cells including intestinal cells (Laburthe & Couvineau, 1988), the effect of VIP on Cl^- current was examined. Paneth cells equilibrated with NaCl solutions were found to respond to VIP (250 nM) with activation of Cl^- currents in a completely reversible manner,

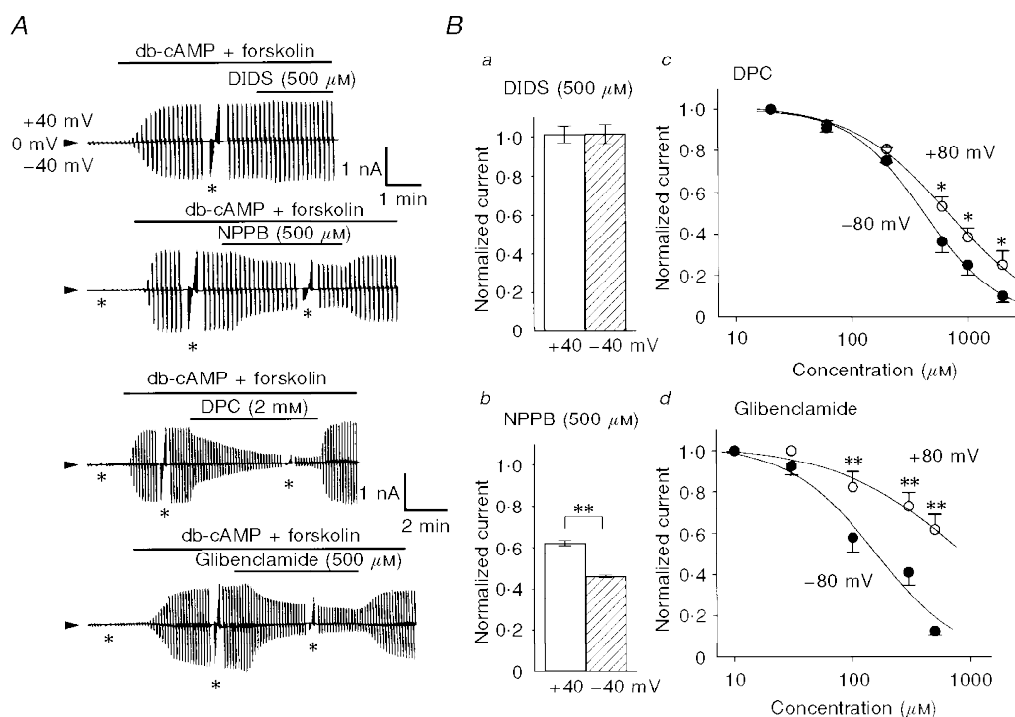


Figure 5. Effects of Cl^- channel blockers on cAMP-activated Cl^- currents

Whole-cell recordings were performed in single Paneth cells equilibrated with NaCl solutions. A, representative records before and after cAMP stimulation ($500 \mu\text{M}$ db-cAMP and $20 \mu\text{M}$ forskolin) and drug application (indicated by horizontal bars) during application of alternating pulses or step pulses. The gain of the chart recorder was changed by one-half during the step pulses (asterisks). The upper time scale applies to both the top and second traces, and the lower scale to both the third and bottom traces. B, mean values of normalized peak currents in the presence of $500 \mu\text{M}$ DIDS (a), $500 \mu\text{M}$ NPPB (b), various concentrations of DPC (c) or glibenclamide (d) against control currents in the absence of drugs at $\pm 40 \text{ mV}$ or $\pm 80 \text{ mV}$. Error bars represent s.e.m. ($n = 4-8$). * $P < 0.05$ and ** $P < 0.01$, significant difference between data recorded at $+40$ and -40 mV , or those at $+80$ and -80 mV . Curves in c and d represent the best fits to the Hill equation. The Hill coefficients for DPC were 1.35 ± 0.13 at -80 mV and 1.03 ± 0.09 at $+80 \text{ mV}$ and those for glibenclamide were 1.18 ± 0.33 at -80 mV and 0.80 ± 0.23 at $+80 \text{ mV}$.

as shown in Fig. 7*Aa*. VIP-induced outward currents showed little time and voltage dependence, whereas the inward currents exhibited weak but distinct inactivation kinetics at large negative potentials (Fig. 7*Ac*). The fast and slow time constants of inactivation were 20.1 ± 1.5 and 335.5 ± 63.7 ms, respectively, at 150 mM extracellular Cl^- and -80 mV, and were not significantly different from those of cAMP-activated Cl^- currents (Fig. 4). The instantaneous $I-V$ curve was virtually linear (Fig. 7*Ad*). When $[\text{Cl}^-]_o$ was reduced from 150 to 50 mM, the V_{rev} shifted by $+29.3 \pm 1.5$ mV ($n = 7$), indicating Cl^- selectivity (cf. chloride equilibrium potential shift of $+27.7$ mV). The VIP response was concentration dependent, as shown in Fig. 7*Ae*, with a half-maximal effective concentration of 1.70 ± 0.12 nM, suggesting an involvement of a high-affinity VIP receptor. Similar Cl^- current responses were also induced by stimulation with $1 \mu\text{M}$ secretin (data not shown, $n = 6$).

The involvement of G proteins in the VIP response was examined by incorporating GDP β S or GTP γ S into the pipette solution. As shown in Fig. 7*B*, VIP-induced Cl^- current activation was largely abolished by $100 \mu\text{M}$ GDP β S (*a* and *c*). However, GDP β S failed to affect Cl^- current activation by a cAMP cocktail (data not shown, $n = 3$). In contrast, $100 \mu\text{M}$ GTP γ S failed to inhibit the VIP response (*b* and *c*); however, it inhibited deactivation of the current after washout of VIP (*b*). Prior treatment with H-89 for over 30 min remarkably suppressed the VIP response (*c*), suggesting the involvement of cAMP-dependent phosphorylation in the VIP-induced channel activity.

Assessment of CFTR mRNA expression in Paneth cells

To assess the expression of CFTR in Paneth cells, the single-cell RT-PCR technique was adopted. After recording cAMP-activated Cl^- currents under the whole-cell mode in Paneth cells in isolated crypts stained with Neutral Red (Fig. 8*A*), negative pressure was applied to the patch pipette to harvest the cytosol. During suction, the cell was found to shrink, and the cytoplasmic contents including stained granules were actually found to be sucked up into the patch pipette (Fig. 8*B*). The cytosol thus collected was subjected to RT-PCR with PCR primers for G-3-PDH and CFTR. In all single Paneth cells examined ($n = 14$), G-3-PDH mRNA was consistently identified (Fig. 8*C*; Single cell). In contrast, CFTR mRNA could not be identified in thirteen of fourteen Paneth cells (Fig. 8*D*; Single cell). To increase the copy number of the CFTR gene, the cytoplasmic contents accumulated from three Paneth cells were subjected to RT-PCR studies. Again, however, we failed to detect CFTR mRNA (data not shown, $n = 2$).

At the whole-crypt level, even after a 10^{-5} times dilution, mRNA expression of not only G-3-PDH but also CFTR was consistently observed by RT-PCR analysis (Fig. 8*C* and *D*; Whole crypt). However, no signal was detected from the same sample without addition of reverse transcriptase (RT $-$) and from bath solution which had been collected during the above single-cell RT-PCR experiments (Bath solution). The cDNA content in this sample after 10^{-5} times dilution was evaluated to be 10.1 pg by spectrophotometry.

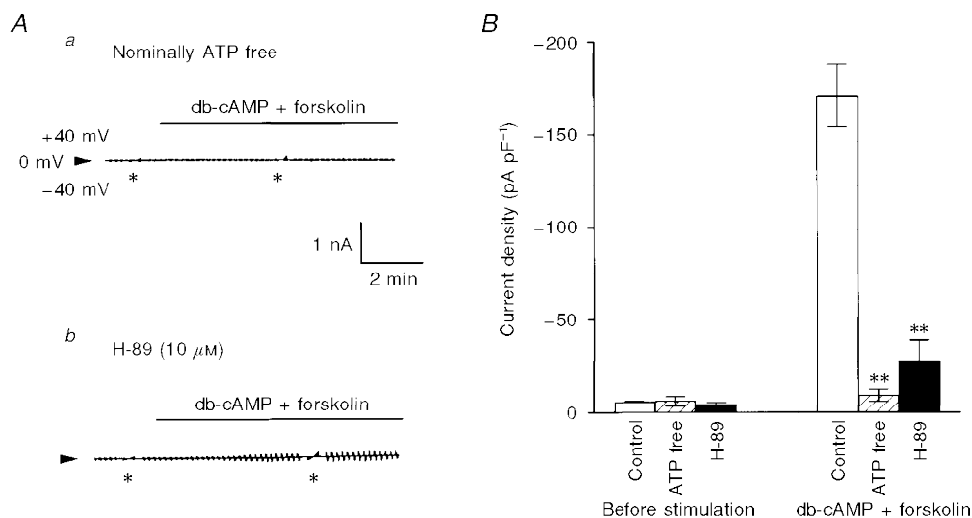


Figure 6. Sensitivity of cAMP-activated Cl^- currents to intracellular ATP removal and to extracellular H-89 administration

Whole-cell recordings were performed in single Paneth cells equilibrated with NaCl solutions. *A*, representative records before and after cAMP stimulation ($500 \mu\text{M}$ db-cAMP and $20 \mu\text{M}$ forskolin) using nominally ATP-free pipette solution (*a*) or after addition (over 30 min) of $10 \mu\text{M}$ H-89 in the pipette solution (*b*). Asterisks indicate application of step pulses from -100 to $+100$ mV in 20 mV increments (see legend to Fig. 2). *B*, effects of nominally ATP-free pipette solution and H-89 in the intracellular pipette solution on the mean current densities recorded at -40 mV ($n = 6-31$). Error bars represent s.e.m. ** $P < 0.01$, significantly different from the control value after stimulation.

Since the cDNA content in an ordinary mammalian cell is thought to be around 50 pg (Sucher & Deitcher, 1995), it is unlikely that failure of CFTR mRNA amplification by single-cell RT-PCR was due to insufficient amount of the sample cDNA.

Assessment of CFTR protein expression in Paneth cells

In order to detect the expression of CFTR, protein immunocytochemical studies were performed in isolated villi and crypts using polyclonal antibody against an octapeptide corresponding to the R domain of guinea-pig CFTR. Immunofluorescence signals were consistently detected with anti-CFTR antibodies but not with non-immune rabbit serum or purified rabbit IgG. As shown in Fig. 9A–F, CFTR-positive cells were found to be scattered from the villi to the crypts, and the fluorescence signal was detected throughout the entire cell. This result is in good agreement with the previous finding in human and rat proximal small intestine (Ameen *et al.* 1995). Distribution of

such a unique subset of enterocytes with a high level of intracellular CFTR appeared to be slightly denser at the lower part of villi (Fig. 9D) than at the upper villus (Fig. 9B) and at the crypt (Fig. 9F). At the crypt base, where Paneth cells are located, CFTR-rich cells could not be observed, and the fluorescence signal was not higher than that of the background level observed in the negative control (data not shown).

Immunoprecipitation studies showed that the guinea-pig intestinal epithelium expressed two types of protein, 200 and 135 kDa, which were reactive to the polyclonal anti-CFTR antibody, as demonstrated in Fig. 9G, but not to purified rabbit IgG. Bands at 135 and 200 kDa are close to those previously reported (Gregory *et al.* 1990; Hoogeveen *et al.* 1991) and may represent the core-glycosylated form and the fully glycosylated form of CFTR, respectively.

Therefore, it appears that almost all the Paneth cells do not express CFTR, whereas almost all the cells exhibit a cAMP-activated Cl^- conductance.

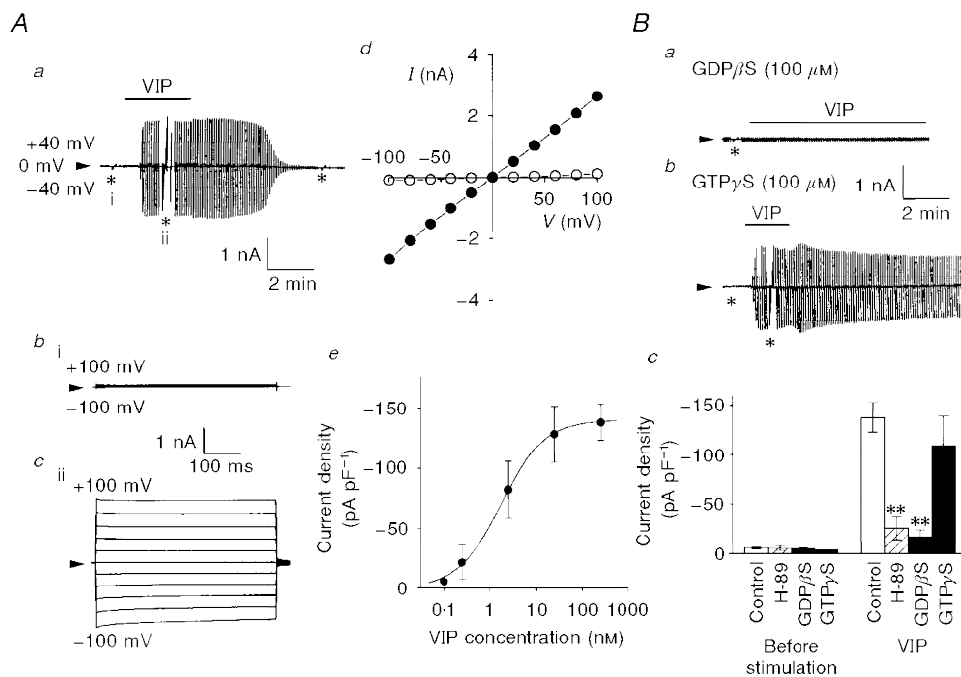


Figure 7. VIP-induced activation of whole-cell Cl^- currents

Whole-cell recordings were performed in single Paneth cells equilibrated with NaCl solutions. *A*, VIP-induced Cl^- currents. *a*, representative record before and after stimulation with 250 nM VIP (indicated by the horizontal line) during application of alternating pulses or step pulses (*; i and ii). The gain of the chart recorder was changed by one-half when step pulses were applied. *b* and *c*, expanded traces of the current responses (i and ii in *a*) to step pulses before (i) and after (ii) VIP stimulation. *d*, peak $I-V$ relationships before (○) and after (●) VIP stimulation for data shown in *c*. *e*, concentration-response curve for VIP. Each symbol represents the mean \pm s.e.m. of VIP-induced peak current density of 4–7 experiments. The curve represents the best fit to the Hill equation with a Hill coefficient of 0.90 ± 0.07 . *B*, effects of GDP β S, GTP γ S and H-89 on VIP-induced Cl^- currents. *a* and *b*, representative records before and after stimulation with VIP during intracellular loading with 100 μM GDP β S or GTP γ S, respectively. Pulse protocol same as that in *A*. *c*, mean peak current density recorded at -40 mV before and after stimulation with VIP without (Control, $n=7$) and with intracellular loading with H-89 ($n=5$), GDP β S ($n=6$) or GTP γ S ($n=5$) for over 30 min. Error bars represent s.e.m. ** $P < 0.01$, significantly different from the control value after stimulation.

DISCUSSION

Novel type of cAMP-activated Cl⁻ channel in Paneth cells

The molecular identity and functional characteristics of Cl⁻ channels in the mammalian small intestine, which is a site of absorption and secretion of Cl⁻, are largely unknown. So far only a few patch-clamp studies on small intestinal Cl⁻ channels have been reported. cAMP-insensitive, outwardly rectifying Cl⁻ channels, which exhibit a low field strength anion selectivity, were found in the basolateral membrane of enterocytes isolated from villi of the guinea-pig small intestine (Sepúlveda *et al.* 1991). In a human small intestinal epithelial cell line, Intestine 407, volume-sensitive outwardly rectifying Cl⁻ channels and Ca²⁺-activated Cl⁻ channels have consistently been found (Okada, 1997). The electrical coupling via gap junctions between undifferentiated enterocytes has prevented precise voltage-clamp studies of the isolated crypt. Even in the isolated crypt, however, the

patch-clamp voltage-clamp study can be applied to Paneth cells which lack gap junctions.

The present patch-clamp study demonstrated, for the first time, that Paneth cells possess cAMP-activated Cl⁻ channels characterized by the following macroscopic properties: (1) ohmic *I-V* relationship, (2) intracellular ATP requirement, (3) PKA dependence, (4) anion selectivity with a moderate field strength Type III sequence (Br⁻ > Cl⁻ > I⁻ > F⁻), (5) blockage by I⁻, (6) insensitivity to DIDS, (7) sensitivity to DPC and NPPB, (8) sensitivity to glibenclamide, (9) weak inactivation at large negative potentials, and (10) extracellular [Cl⁻] dependence of channel activity and inactivation gating. Most of the above properties (points 1–7) resemble the macroscopic properties of the CFTR Cl⁻ channel (Fuller & Benos, 1992). However, cAMP-activated Cl⁻ currents in Paneth cells exhibited much lower sensitivity to glibenclamide (IC₅₀: 150–260 μM at -80 to -40 mV) than epithelial (IC₅₀: 15 μM at -50 mV;

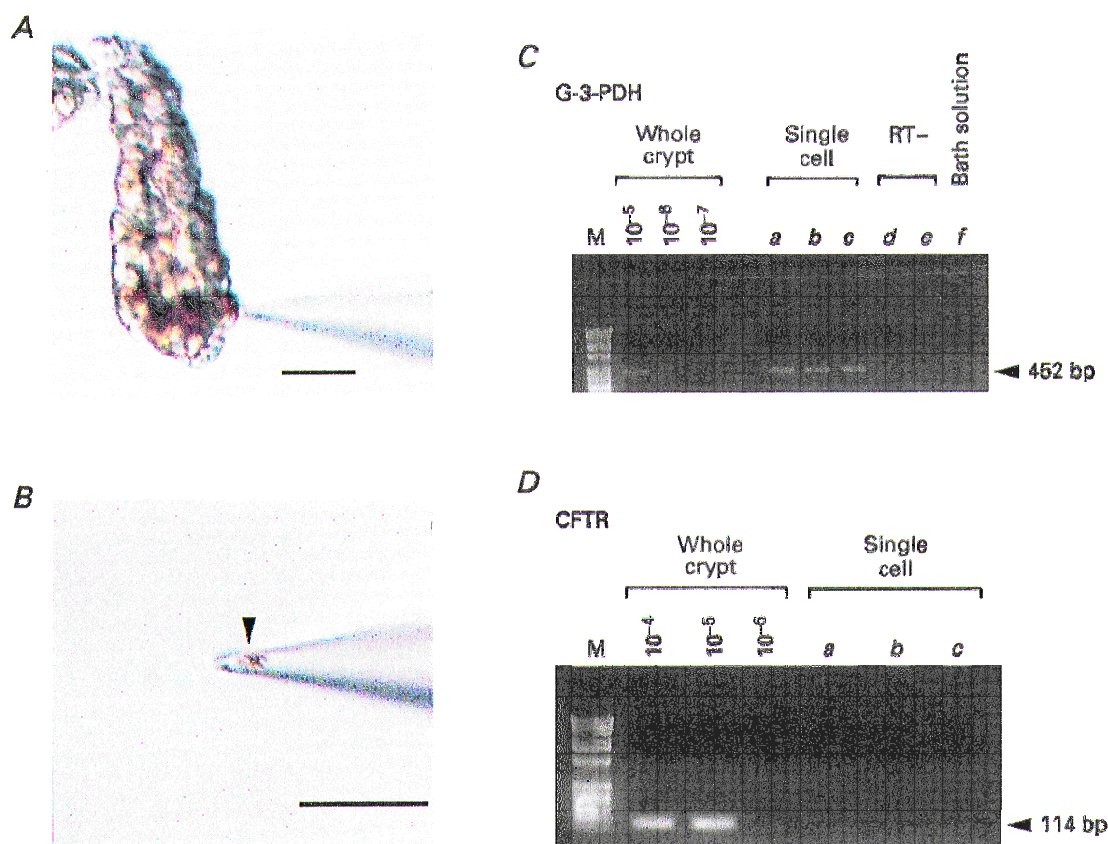


Figure 8. Single-cell RT-PCR analysis for CFTR mRNA expression

A, micrograph of a crypt stained with Neutral Red during whole-cell recordings in a Paneth cell. Scale bar, 30 μm. B, patch pipette containing the cytoplasmic contents which were sucked up from a Paneth cell after whole-cell recording. Scale bar, 30 μm. C, gel analysis of G-3-PDH-specific PCR product (predicted to be 452 bp) from a whole crypt after dilution (10⁻⁵, 10⁻⁶ or 10⁻⁷ times) or single Paneth cells (a–c). As a negative control, the same procedures were conducted using single-cell cytoplasm without reverse transcriptase (RT–; d and e) or using bath solution from the same experiments (f). A molecular weight marker (ϕX174 DNA/*Hae*III fragment; Gibco BRL) is shown in the left-hand lane (M). D, gel analysis of CFTR-specific PCR product (predicted to be 114 bp) from a whole crypt after dilution (10⁻⁴, 10⁻⁵ or 10⁻⁶ times) or single Paneth cells (a–c).

Sheppard & Robinson, 1997) and cardiac (IC_{50} : $30 \mu\text{M}$ at -10 mV ; Tominaga *et al.* 1995) CFTR Cl^- channel currents. Its time- and voltage-dependent inactivation was also distinct from that of CFTR channel current. Moreover, relevant evidence for the molecular expression of CFTR could not be obtained in the present study.

The Paneth cell Cl^- currents share $[\text{Cl}^-]_o$ -dependent inactivation kinetics with those of the ClC-0 Cl^- channel (Pusch *et al.* 1995) which was cloned from *Torpedo* electric organ and shown to have a consensus phosphorylation site for PKA (Jentsch *et al.* 1990). However, other ClC-0 properties such as outward rectification, anion selectivity of $\text{Cl}^- > \text{Br}^- > \text{I}^-$ and DIDS sensitivity are distinct from those of cAMP-activated Cl^- channels expressed in guinea-pig Paneth cells. Some of the properties of the $\text{ClC-2G}(2\alpha)$ Cl^- channel, which was cloned from a rabbit gastric cDNA library and shown to have potential PKA phosphorylation sites, are similar to those of the Paneth cell Cl^- channel, for example, ohmic I - V relationship and PKA-induced activation (Malinowska *et al.* 1995). However, the anion selectivity ($\text{I}^- > \text{Cl}^-$) of $\text{ClC-2G}(2\alpha)$ is distinct from that of the Paneth cell Cl^- channel. Moreover, mRNA expression

of ClC-0 and $\text{ClC-2G}(2\alpha)$ has not been observed in the mammalian small intestine.

PKA-activated Cl^- channels in rat and mouse choroid plexus epithelial cells have recently been clearly demonstrated to be distinct from CFTR by the method of RNA *in situ* hybridization in the normal rat (Kibble *et al.* 1996) and by employing the cystic fibrosis transgenic mouse (Kibble *et al.* 1997). The properties of the choroid plexus channel currents differ from those of Paneth cell cAMP-activated Cl^- current in their inward rectification, anion selectivity sequence of $\text{I}^- > \text{Cl}^- > \text{Br}^-$ and DIDS sensitivity. PKA-activated Cl^- channel currents were also found in isolated *Necturus* enterocytes (Giraldez *et al.* 1989). Their outward rectification, low field strength anion selectivity and sensitivity to a stilbene-derivative Cl^- channel blocker are at variance with the properties of the Paneth cell PKA-regulated Cl^- current.

Prompt changes in the cAMP-activated Cl^- current profile were induced by the addition of DPC or glibenclamide to the basolateral bathing solution or by the reduction of basolateral Cl^- concentration. These results suggest that the Paneth cell Cl^- channel resides on the basolateral membrane but not on the luminal membrane which is not readily

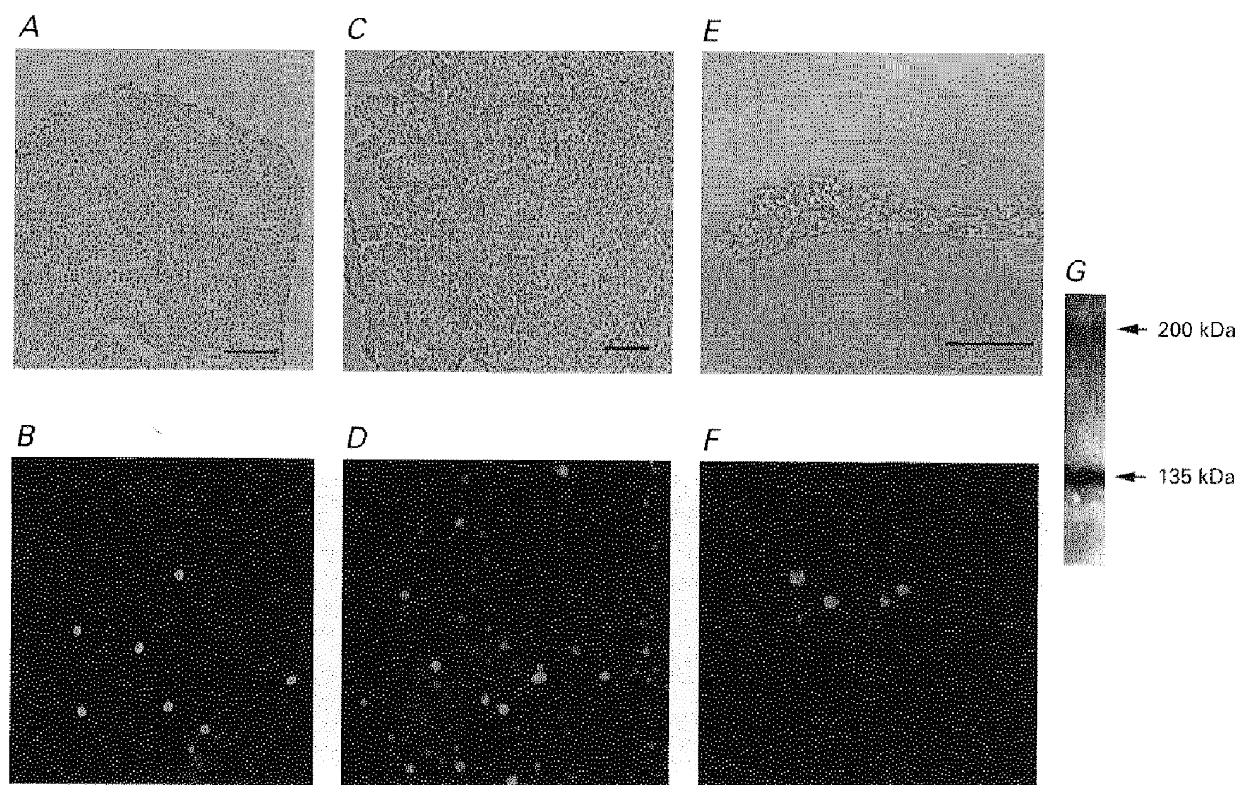


Figure 9. Immunocytochemistry and immunoprecipitation analysis for CFTR protein expression

A, *C* and *E*, light micrographs of a villus fragment (*A*), a fragment consisting of a lower villus and upper or whole crypts (*C*) and a whole-crypt fragment (*E*) isolated from guinea-pig small intestine. Scale bars, $50 \mu\text{m}$. *B*, *D* and *F*, indirect immunofluorescence micrographs of epithelial fragments corresponding to *A*, *C* and *E*, respectively. Immunocytochemistry was performed with anti-CFTR antibody. *G*, immunoprecipitation of CFTR. Isolated epithelial fragments were solubilized using detergent and CFTR was immunoprecipitated with anti-CFTR antibody. Data represent duplicate experiments.

exposed to the bathing solution. This inference may also be supported by the fact that closure of the open end of crypt glands did not affect the amplitude of cAMP-activated Cl^- current at all. To determine precisely the location of the channel, however, further investigations including single-channel studies are needed.

Taken together, it appears that Paneth cells possess cAMP-activated Cl^- channels which are distinct from any known cAMP- or PKA-activated Cl^- channels, although the single-channel properties remain to be investigated.

Molecular expression of CFTR in the guinea-pig small intestine

Recent studies using cystic fibrosis mouse models made by CFTR gene targeting clearly showed that CFTR is responsible for the small intestinal Cl^- secretion (Grubb & Gabriel, 1997). *In situ* hybridization studies in rat and human small intestines have shown that distribution of CFTR mRNA is greater in the crypt than in the villus (Trezise & Buchwald, 1991; Strong *et al.* 1994). Uniform expression of CFTR mRNA was suggested in all the crypt enterocytes including Paneth cells in the human duodenum and jejunum (Strong *et al.* 1994). However, the present single-cell RT-PCR study failed to amplify CFTR mRNA in almost all the guinea-pig Paneth cells.

Immunocytochemical studies have so far provided contradictory information about the distribution of CFTR protein in the mammalian small intestine. Protein expression was found in the crypt of human small intestine by Crawford *et al.* (1991), and its intense expression was found in the apical region of mouse small intestinal crypts by French *et al.* (1996). In contrast, the strongest expression was found in the endoplasmic reticulum of goblet cells in human duodenum (Hoogeveen *et al.* 1991). Recently, Ameen *et al.* (1995) showed that there are a small number of unique enterocytes expressing a very high level of CFTR protein in the rat and human proximal small intestine. This subpopulation was found to be scattered through villi to crypts but not at the crypt base where Paneth cells reside. The present immunofluorescence study in villi and crypts isolated from guinea-pig small intestine was in good agreement with the findings of Ameen *et al.* (1995). The role of CFTR in such a unique subset of enterocytes remains to be elucidated. However, it is likely that CFTR protein is not the molecular identity for the cAMP-activated Cl^- conductance which was consistently found in guinea-pig Paneth cells.

Physiological significance

Molecular expression of the VIP receptor has been shown in the small intestine of rat (Ishihara *et al.* 1992) and human (Sreedharan *et al.* 1995) by Northern blot analysis. Functional expression of VIP receptors coupled to adenylyl cyclase through a G_s protein has also been shown by binding assay and adenylyl cyclase assay in the plasma membrane of crypt enterocytes of human jejunum (Salomon *et al.* 1993). In the present study, the functional expression of VIP

receptors was demonstrated for the first time by patch clamp in Paneth cells of guinea-pig small intestine. The effects of GDP β S and GTP γ S indicate an involvement of G proteins in the VIP receptor response. Paneth cells are known to respond to β -adrenergic agonists, which should increase intracellular [cAMP], with lysozyme secretion (Olson & Erlandsen, 1981). Therefore, there is a possibility that a cAMP increase induced by stimulation of VIP receptors is involved not only in activation of Cl^- conductance but also in the regulation of exocytosis in Paneth cells.

Paneth cells are thought to play a key role in host defence of the bowel by releasing a number of bioactive contents within the granules into the lumen (Ouellette, 1997). The mechanism of exocytosis in Paneth cells is largely obscure. However, intracellular vesicular transport and cell volume regulation can be expected to occur before, during and after the exocytotic event. In some cell types, it is known that the cAMP-dependent Cl^- conductance plays essential roles in exocytotic membrane recycling (Bradbury *et al.* 1992) and cell volume regulation (Okada, 1997). Thus, it is possible that the cAMP-activated Cl^- channel activity in Paneth cells is associated with the exocytotic process. Also, there is a possibility that the Cl^- channel mediates net Cl^- transport through Paneth cells. However, the exact roles of the cAMP-activated Cl^- channel and the VIP receptor expressed in Paneth cells await further investigation.

- AMEEN, N. A., ARDITO, T., KASHGARIAN, M. & MARINO, C. R. (1995). A unique subset of rat and human intestinal villus cells express the cystic fibrosis transmembrane conductance regulator. *Gastroenterology* **108**, 1016–1023.
- BEAR, C. E. & REYES, E. F. (1992). cAMP-activated chloride conductance in the colonic cell line, Caco-2. *American Journal of Physiology* **262**, C251–256.
- BJERKNES, M., CHENG, H. & ERLANDSEN, S. (1985). Functional gap junctions in mouse small intestinal crypts. *Anatomical Record* **212**, 364–367.
- BRADBURY, N. A., JILLING, T., BERTA, G., SORSCHER, E. J., BRIDGES, R. J. & KIRK, K. L. (1992). Regulation of plasma membrane recycling by CFTR. *Science* **256**, 530–532.
- CRAWFORD, I., MALONEY, P. C., ZEITLIN, P. L., GUGGINO, W. B., HYDE, S. C., TURLEY, H., GATTER, K. C., HARRIS, A. & HIGGINS, C. F. (1991). Immunocytochemical localization of the cystic fibrosis gene product CFTR. *Proceedings of the National Academy of Sciences of the USA* **88**, 9262–9266.
- DIAMOND, G., SCANLIN, T. F., ZASLOFF, M. A. & BEVINS, C. L. (1991). A cross-species analysis of the cystic fibrosis transmembrane conductance regulator. Potential functional domains and regulatory sites. *Journal of Biological Chemistry* **266**, 22761–22769.
- FRENCH, P. J., VAN DOORNINCK, J. H., PETERS, R. H. P. C., VERBEEK, E., AMEEN, N. A., MARINO, C. R., DE JONGE, H. R., BIJMAN, J. & SCHOLTE, B. J. (1996). A Δ F508 mutation in mouse cystic fibrosis transmembrane conductance regulator results in a temperature-sensitive processing defect in vivo. *Journal of Clinical Investigation* **98**, 1304–1312.
- FULLER, C. M. & BENOS, D. J. (1992). CFTR! *American Journal of Physiology* **263**, C267–286.

- GIRALDEZ, F., MURRAY, K. J., SEPÚLVEDA, F. V. & SHEPPARD, D. N. (1989). Characterization of a phosphorylation-activated Cl⁻-selective channel in isolated *Necturus* enterocytes. *Journal of Physiology* **416**, 517–537.
- GREGORY, R. J., CHENG, S. H., RICH, D. P., MARSHALL, J., PAUL, S., HEHIR, K., OSTEDGAARD, L., KLINGER, K. W., WELSH, M. J. & SMITH, A. E. (1990). Expression and characterization of the cystic fibrosis transmembrane conductance regulator. *Nature* **347**, 382–386.
- GRUBB, B. R. & GABRIEL, S. E. (1997). Intestinal physiology and pathology in gene-targeted mouse models of cystic fibrosis. *American Journal of Physiology* **273**, G258–266.
- HOOGVEEN, A. T., KEULEMANS, J., WILLEMSSEN, R., SCHOLTE, B. J., BIJMAN, J., EDIXHOVEN, M. J., DE JONGE, H. R. & GALJAARD, H. (1991). Immunological localization of cystic fibrosis candidate gene products. *Experimental Cell Research* **193**, 435–437.
- ISHIHARA, T., SHIGEMOTO, R., MORI, K., TAKAHASHI, K. & NAGATA, S. (1992). Functional expression and tissue distribution of a novel receptor for vasoactive intestinal polypeptide. *Neuron* **8**, 811–819.
- JENTSCH, T. J., STEINMEYER, K. & SCHWARZ, G. (1990). Primary structure of *Torpedo marmorata* chloride channel isolated by expression cloning in *Xenopus* oocytes. *Nature* **348**, 510–514.
- KIBBLE, J. D., GARNER, C., COLLEDGE, W. H., BROWN, S., KAJITA, H., EVANS, M. & BROWN, P. D. (1997). Whole-cell Cl⁻ conductances in mouse choroid plexus epithelial cells do not require CFTR expression. *American Journal of Physiology* **272**, C1899–1907.
- KIBBLE, J. D., TREZISE, A. E. O. & BROWN, P. D. (1996). Properties of the cAMP-activated Cl⁻ current in choroid plexus epithelial cells isolated from the rat. *Journal of Physiology* **496**, 69–80.
- LABURTHE, M. & COUVINEAU, A. (1988). Molecular analysis of vasoactive intestinal peptide receptors. *Annals of the New York Academy of Sciences* **527**, 296–313.
- LENCER, W. I., CHEUNG, G., STROHMEIER, G. R., CURRIE, M. G., OUELLETTE, A. J., SELSTED, M. E. & MADARA, J. L. (1997). Induction of epithelial chloride secretion by channel-forming cryptidins 2 and 3. *Proceedings of the National Academy of Sciences of the USA* **94**, 8585–8589.
- MENICHOLO, C. M., BROWN, C. D. A. & TURNBERG, L. A. (1994). Na–K–Cl cotransport in villus and crypt cells from rat duodenum. *American Journal of Physiology* **267**, G1004–1011.
- MALINOWSKA, D. H., KUPERT, E. Y., BAHINSKI, A., SHERRY, A. M. & CUPPOLETTI, J. (1995). Cloning, functional expression, and characterization of a PKA-activated gastric Cl⁻ channel. *American Journal of Physiology* **268**, C191–200.
- OKADA, Y. (1997). Volume expansion-sensing outward-rectifier Cl⁻ channel: fresh start to the molecular identity and volume sensor. *American Journal of Physiology* **273**, C755–789.
- OLSON, R. E. & ERLANDSEN, S. L. (1981). Paneth cell function: The effects of cholinergic and adrenergic drugs on lysozyme secretion. *Anatomical Record* **199**, 186A (abstract).
- OUELLETTE, A. J. (1997). Paneth cells and innate immunity in the crypt microenvironment. *Gastroenterology* **113**, 1779–1784.
- PUSCH, M., LUDEWIG, U., REHFELDT, A. & JENTSCH, T. J. (1995). Gating of the voltage-dependent chloride channel ClC-0 by the permeant anion. *Nature* **373**, 527–531.
- RAPPOLEE, D. A., MARK, D., BANDA, M. J. & WERB, Z. (1988). Wound macrophages express TGF- α and other growth factors in vivo: Analysis by mRNA phenotyping. *Science* **241**, 708–712.
- SALOMON, R., COUVINEAU, A., ROUYER-FESSARD, C., VOISIN, T., LAVALLÉE, D., BLAIS, A., DARMOUL, D. & LABURTHE, M. (1993). Characterization of a common VIP-PACAP receptor in human small intestinal epithelium. *American Journal of Physiology* **264**, E294–300.
- SEPÚLVEDA, F. V., FARGON, F. & MCNAUGHTON, P. A. (1991). K⁺ and Cl⁻ currents in enterocytes isolated from guinea-pig small intestinal villi. *Journal of Physiology* **434**, 351–367.
- SHEPPARD, D. N. & ROBINSON, K. A. (1997). Mechanism of glibenclamide inhibition of cystic fibrosis transmembrane conductance regulator Cl⁻ channels expressed in a murine cell line. *Journal of Physiology* **503**, 333–346.
- SREEDHARAN, S. P., HUANG, J.-X., CHEUNG, M.-C. & GOETZL, E. J. (1995). Structure, expression, and chromosomal localization of the type I human vasoactive intestinal peptide receptor gene. *Proceedings of the National Academy of Sciences of the USA* **92**, 2939–2943.
- STRONG, T. V., BOEHM, K. & COLLINS, F. S. (1994). Localization of cystic fibrosis transmembrane conductance regulator mRNA in the human gastrointestinal tract by in situ hybridization. *Journal of Clinical Investigation* **93**, 347–354.
- SUCHER, N. J. & DEITCHER, D. L. (1995). PCR and patch-clamp analysis of single neurons. *Neuron* **14**, 1095–1100.
- SULLIVAN, S. K. & FIELD, M. (1991). Ion transport across mammalian small intestine. In *Handbook of Physiology*, section 6, *The Gastrointestinal System*, vol. IV, *Intestinal Absorption and Secretion*, ed. FIELD, M. & FRIZZELL, R. A., pp. 287–301. American Physiological Society, Bethesda, MD, USA.
- TABCHARANI, J. A., LOW, W., ELIE, D. & HANRAHAN, J. W. (1990). Low-conductance chloride channel activated by cAMP in the epithelial cell line T₈₄. *FEBS Letters* **270**, 157–164.
- TOMINAGA, M., HORIE, M., SASAYAMA, S. & OKADA, Y. (1995). Glibenclamide, an ATP-sensitive K⁺ channel blocker, inhibits cardiac cAMP-activated Cl⁻ conductance. *Circulation Research* **77**, 417–423.
- TREZISE, A. E. O. & BUCHWALD, M. (1991). *In vivo* cell-specific expression of the cystic fibrosis transmembrane conductance regulator. *Nature* **353**, 434–437.
- TSUMURA, T., HAZAMA, A., OIKI, S., UEDA, S. & OKADA, Y. (1997). CFTR-type Cl⁻ currents in guinea pig Paneth cells. *Japanese Journal of Physiology* **47**, suppl., S123 (abstract).
- TSUMURA, T., OIKI, S., UEDA, S., OKUMA, M. & OKADA, Y. (1996). Sensitivity of volume-sensitive Cl⁻ conductance in human epithelial cells to extracellular nucleotides. *American Journal of Physiology* **271**, C1872–1878.
- WALTERS, R. J., O'BRIEN, J. A., VALVERDE, M. A. & SEPÚLVEDA, F. V. (1992). Membrane conductance and cell volume changes evoked by vasoactive intestinal polypeptide and carbachol in small intestinal crypts. *Pflügers Archiv* **421**, 598–605.
- WRIGHT, E. & DIAMOND, J. M. (1977). Anion selectivity in biological systems. *Physiological Reviews* **57**, 109–156.

Acknowledgements

This work was supported by a Grant-in-Aid for Scientific Research and by a grant for Priority Areas of 'Channel-Transporter Correlation' (07276 104) from the Ministry of Education, Science and Culture of Japan. The authors are grateful to A. F. James (King's College, London, UK) for reading the manuscript, to A. Satoh (Asahikawa Medical College, Japan) for the suggestion about Paneth cell identification, to S. Morishima for advice and help, to M. Ohara and A. Hattori for technical assistance and to M. Takazawa for secretarial help.

Corresponding author

Y. Okada: Department of Cellular and Molecular Physiology, National Institute for Physiological Sciences, Myodaiji-cho, Okazaki 444-8585, Japan.

Email: okada@nips.ac.jp